

Computational Study of Metal Free Alcohol Dehydrogenation Employing Frustrated Lewis Pairs

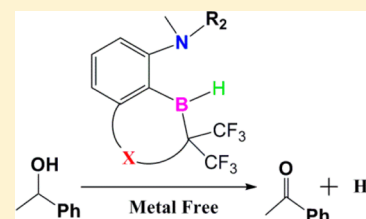
Manoj V. Mane,[†] Masood A. Rizvi,[‡] and Kumar Vanka^{*,†}

[†]Physical Chemistry Division, National Chemical Laboratory, Dr. Homi Bhabha Road, Pashan, Pune, Maharashtra 411 008, India

[‡]Department of Chemistry, University of Kashmir, Hazratbal, Srinagar, 190006 J&K, India

S Supporting Information

ABSTRACT: The catalysis of acceptorless alcohol dehydrogenation (AAD) is an important area of research. Transition metal-based systems are known to be effective catalysts for this reaction, but developing metal free catalytic systems would lead to highly desirable cheaper and greener alternatives. With this in mind, this computational study investigates design strategies that can lead to metal free frustrated Lewis pairs (FLPs) that can be employed for AAD catalysis. A careful study of 36 different proposed FLP candidates reveals that several new FLPs can be designed from existing, experimentally synthesized FLPs that can rival or be even better than state-of-the-art transition metal-based systems in catalyzing the alcohol dehydrogenation process.



INTRODUCTION

Alcohol dehydrogenation is often used to activate alcohols to the more reactive ketones or aldehydes.^{1–4} Today, the demand for renewable energy sources has led to significant interest^{5–8} in utilizing alcohol dehydrogenation for the production of H₂ from biomass or its fermentation products, usually employing transition metal catalysts.^{9–12} A variety of transition metal catalysts such as rhodium, iridium, and ruthenium have been reported^{13–22} for this process, with well-known hydrogen acceptors such as O₂, H₂O₂, and acetones. Acceptorless alcohol dehydrogenation (AAD), on the other hand, is less common^{1–4,11,23–25} but is useful, particularly in terms of H₂ production and atom economy. In this regard, the work of Yamaguchi, Fujita, and their co-workers^{26,27} is significant, because they have developed a new iridium metal complex that catalyzes alcohol dehydrogenation efficiently under mild conditions without requiring acceptors, thus being the most promising AAD catalyst developed to date.

The mechanism for the AAD catalysis by the iridium complex of Yamaguchi et al. has been computationally studied by Wang and co-workers.¹¹ As shown in Figure 1, the mechanism involves three steps: (i) ligand rotation leading to Ir–O bond cleavage to form the reactive intermediate int.1, (ii) hydrogen transfer from the alcohol substrate to form int.3 (through transition state TS), and (iii) release of dihydrogen to regenerate the catalyst. They calculated the overall reaction free energy barrier height¹¹ for 1-phenylethanol dehydrogenation to be 30.0 kcal/mol.

While the experimental and computational work on AAD catalysis, discussed above, is significant, it is notable for the fact that it involves a transition metal complex. Transition metal-catalyzed reactions are not ideal because of the use of expensive transition metals, and the production of waste, high cost, and toxicity. To overcome these disadvantages, the substitution of transition metal systems with Main Group systems is an

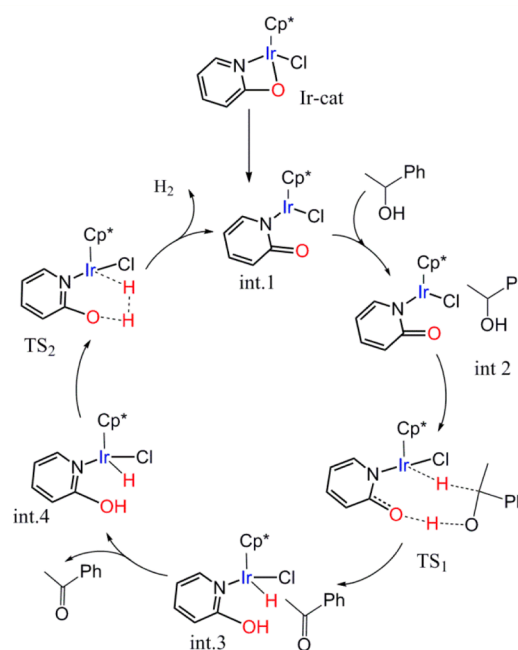


Figure 1. Catalytic cycle for alcohol dehydrogenation.

attractive option, because this can lead to cheap and green catalyst systems. The recent work of Stephan and co-workers²⁸ is important in this context. They have introduced the concept of “frustrated Lewis pairs” (FLPs), which are complexes that contain a Lewis acidic and a Lewis basic center, sterically separated from bonding with each other, leading to latent Lewis acidity and basicity that can be exploited for small molecule activation.^{28–30} FLPs have been employed for the activation of

Received: October 8, 2014

Published: January 23, 2015

dihydrogen^{31,32} and amines.³³ Also, the hydrogenation of C=C,^{34,35} C=N,^{36–38} bulky imine,^{37,39} and C=O⁴⁰ bonds using FLPs has been reported. Furthermore, the dehydrogenation of alcohol to ketone⁴¹ and the dehydrogenation of ammoniaborane^{33,42} by FLPs has also been demonstrated.

With respect to the topic under discussion, AAD, the FLP systems that may be important are phosphinoboranes, which have been studied experimentally^{28,37,38,43–45} and computationally.^{31,41,46–49} Indeed, computational studies have reported the dehydrogenation of alcohol through P/B cooperation in the (tBu)₂P=B(C₆F₅)₂ FLP.⁴¹ However, as shown in Results and Discussion, the barriers in the dehydrogenation process with this system are higher than for the metal-based iridium system¹¹ that has been discussed above. Now, to be truly effective, Main Group-based systems need to have barriers that are similar to, or preferably lower, than the barriers obtained for metal systems. It is therefore imperative that other FLPs be considered that would be as effective as (or more effective than) the existing metal-based system. An effective strategy in this context would be to design more sterically constrained FLPs that would have weaker interaction between the Lewis acidic and basic centers, leading to a lowering of the barriers for the alcohol dehydrogenation process, and thus to more catalytically efficient systems.

With this in mind, we have considered the N/B FLP system shown in Figure 2, which has been experimentally synthesized

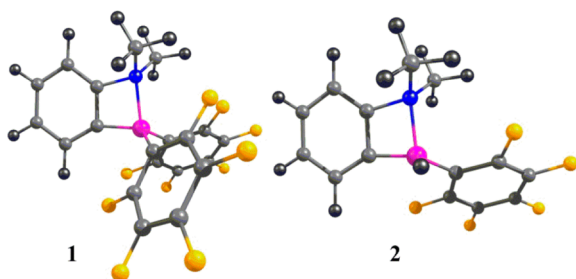


Figure 2. Main Group FLP complexes that have been reported experimentally. The color scheme is as follows: carbon, gray; nitrogen, blue; hydrogen, black; boron, pink; fluorine, yellow.

recently by Chernichenko et al.^{50,51} In this FLP, **1**, and its variant, **2** (see Figure 2), there exists a dative bond between the nitrogen and the boron atoms, which is weaker than the more covalent bond between P and B in the (tBu)₂P=B(C₆F₅)₂ FLP. Furthermore, the coordination of each atom to the phenyl ring ensures greater steric hindrance in this case, which would lead to easier activation of the N–B bond. We have therefore decided to look at **1** and **2** as starting points of a thorough computational investigation into the possibility of employing these complexes, and introduced variations to these complexes, for the efficient dehydrogenation of alcohols. As many as 36 different N/B complexes have been considered, and several promising candidates for the dehydrogenation of the alcohol 1-phenyl ethanol (the same alcohol that had been considered for the iridium-based system¹¹) have been identified. As shown in Results and Discussion, while **1**, **2**, and several of their variants are predicted not to be as effective as the metal-based system, our studies have unearthed some promising candidates that are predicted to be more effective than the metal-based systems for the alcohol dehydrogenation catalysis process.

COMPUTATIONAL DETAILS

The geometry optimizations were conducted employing density functional theory (DFT) with the Turbomole 6.4 suite of programs.⁵² The Perdew, Burke, and Ernzerhof (PBE)⁵³ functional was used for the geometry optimization calculations. The triple- ζ basis set augmented by a polarization function (Turbomole basis set TZVP) was used for all the atoms. In the calculations involving the iridium catalyst, we have employed the def-TZVP basis set for the iridium atom. The resolutions of identity (RI)⁵⁴ along with the multipole accelerated resolution of identity (marij)⁵⁵ approximations were employed for an accurate and efficient treatment of the electronic Coulomb term. To improve the calculation of the energy values, a further correction was made through single-point B3-LYP calculations^{56,57} for the DFT (PBE)-optimized structures. Natural population analysis was conducted to obtain the NBO charges for certain cases described herein, where required. Frequency calculations were conducted at the DFT level to obtain the zero point energy, the internal energy, and entropic contributions (calculated at 298.15 K). Hence, in addition to the ΔH values, ΔG values have also been reported. With regard to the transition states obtained during the investigations of the dehydrogenation process, care was taken to ensure that the obtained transition state structures possessed only one imaginary frequency corresponding to the correct normal mode.

To check whether dispersion effects are important for these systems, we have done full optimizations of structures using Grimme's dispersion corrected functional, B97-D.⁵⁸ The calculations were conducted for the slowest (first) step of the reaction for FLP complexes **3**, **4**, and **16**. Moreover, the full catalytic cycle was determined with this functional for complexes **25** and **30**, which contain large substituents attached to the nitrogen (see Figures S7 and S8 of the Supporting Information). The results, as shown in Table S1 of the Supporting Information, indicate that the values obtained by this TZVP/B97-D approach are quite similar to the corresponding values obtained by our reported TZVP/PBE/B3LYP approach. There is only a slight decrease observed in the barrier height when the TZVP/B97-D approach is employed: the barrier height decreases in the five cases by 1.5–2.8 kcal/mol, while the trends remain the same (see Table S1 of the Supporting Information). Furthermore, as shown in Figures S9 and S10 of the Supporting Information for the case of reactants and transition states for complexes **3** and **4**, the optimized geometries obtained from the TZVP/PBE/B3LYP and the TZVP/B97-D approaches are quite comparably similar.

In short, our calculations reveal that the dispersion corrections are not particularly significant for the systems that we have studied, and therefore, our TZVP/PBE/B3LYP approach is sufficiently robust to handle the newly proposed FLP systems.

RESULTS AND DISCUSSION

The frustrated Lewis pair, **2**, which has been recently synthesized, can be employed for alcohol dehydrogenation. As shown in Figure 3, however, employing such a system would give rise to a barrier of 33.2 kcal/mol for the slowest (first) step of the reaction. This is in contrast to a barrier of 21.9 kcal/mol for the slowest (first) step of the reaction if the iridium catalyst were to be employed (see Figure 4). It is therefore clear that **2** would not be an effective Main Group substitute for the iridium catalyst, which has been employed experimentally to dehydrogenate the alcohol.^{26,27} It is to be noted that the barriers for FLP **1**, discussed in the Introduction, are even higher than those calculated for **2** (see Figure S1 of the Supporting Information), indicating that this would be even poorer at dehydrogenating the alcohol.

However, beginning from **2** as the point of reference, one can modify and design new FLPs that may be superior to **2** as catalysts and even rival the iridium-based catalyst in dehydrogenating the alcohol.

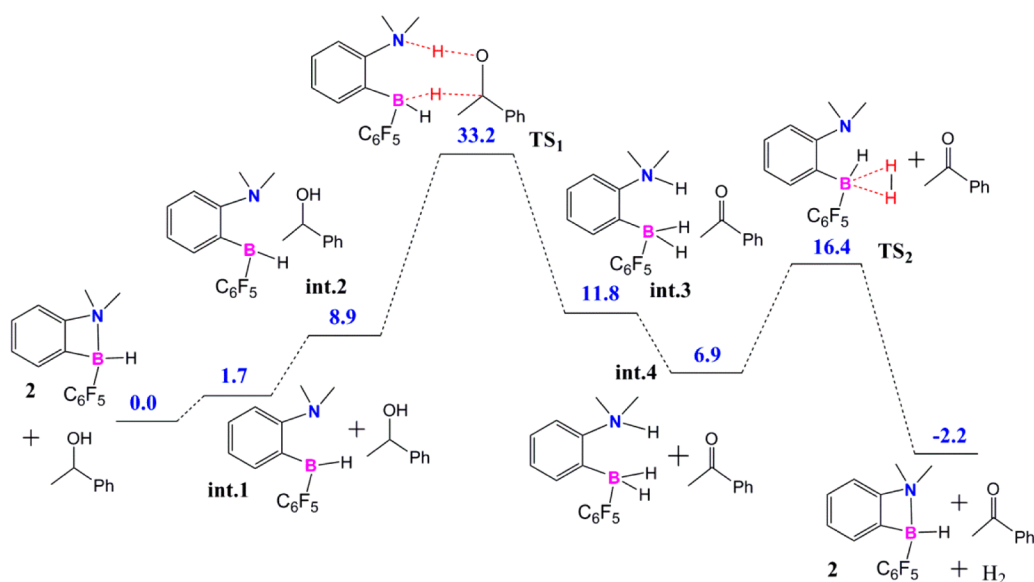


Figure 3. Free energy surface for the alcohol dehydrogenation reaction employing the recently synthesized metal free frustrated Lewis pair complex **2**. All values are in kilocalories per mole.

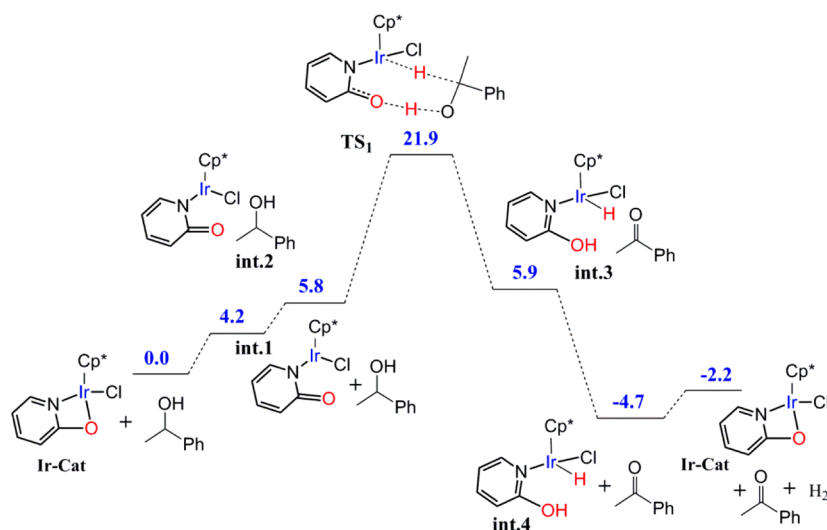


Figure 4. Free energy surface for the alcohol dehydrogenation reaction employing the recently synthesized iridium complex. All values are in kilocalories per mole.

With this in mind, we have designed four strategies for modifying **2**. As shown in Figure 5, the strategies are as follows.

Strategy I. Modify the functional groups on the nitrogen and boron of **2**. The groups modified are denoted as R_1 – R_3 . As shown in Table 2, R_1 has been generally kept as the CH_3 group, while for R_2 , the different groups that have been considered are CH_3 , $\text{C}(\text{CH}_3)_3$, $\text{CH}(\text{CH}_2)_2$, and $\text{N}(\text{CH}_3)_2$; for R_3 , C_6F_5 and $\text{C}(\text{CH}_3)_3$ have been considered as the functional groups. Furthermore, all the corresponding cases with the hydrogens of the phenyl backbone of **2** replaced with fluorine atoms have also been considered.

Strategy II. Modify **2** by adding a linker, $\text{C}(\text{CF}_3)_2$ – CF_2 – CH_2 – CH_2 , between the boron and the backbone phenyl group (see Figure 5). As will be explained below, the reason for adopting this strategy of “sewing” the boron and the back phenyl group together is to reduce the level of interaction between the boron and the nitrogen atoms, thereby sterically increasing the level of frustration in the FLP. Different R_2

groups have been considered for this case, including CH_3 , $\text{C}(\text{CH}_3)_3$, $\text{CH}(\text{CH}_2)_2$, and $\text{N}(\text{CH}_3)_2$. All the corresponding cases with the hydrogens of the phenyl backbone replaced with fluorine atoms have also been considered.

Strategy III. Modify **2** by adding a linker, $\text{C}(\text{CF}_3)_2$ – CF_2 – CF_2 – CF_2 , between the boron and the backbone phenyl group (see Figure 5). This is a variant of strategy II, with the emphasis being on observing how having fluorines in place of hydrogens leads to a change in the alcohol dehydrogenation barrier. Different R_2 groups have been considered for this case, including CH_3 , $\text{C}(\text{CH}_3)_3$, $\text{CH}(\text{CH}_2)_2$, and $\text{N}(\text{CH}_3)_2$.

Strategy IV. Modify **2** by adding a linker, CF_2 – CF_2 – CF_2 – CF_2 , between the boron and the backbone phenyl group (see Figure 5). Different R_2 groups have been considered for this case, including CH_3 , $\text{C}(\text{CH}_3)_3$, $\text{CH}(\text{CH}_2)_2$, and $\text{N}(\text{CH}_3)_2$. All the corresponding cases with the hydrogens of the phenyl backbone replaced with fluorine atoms have also been considered. A possible synthetic strategy for making an FLP

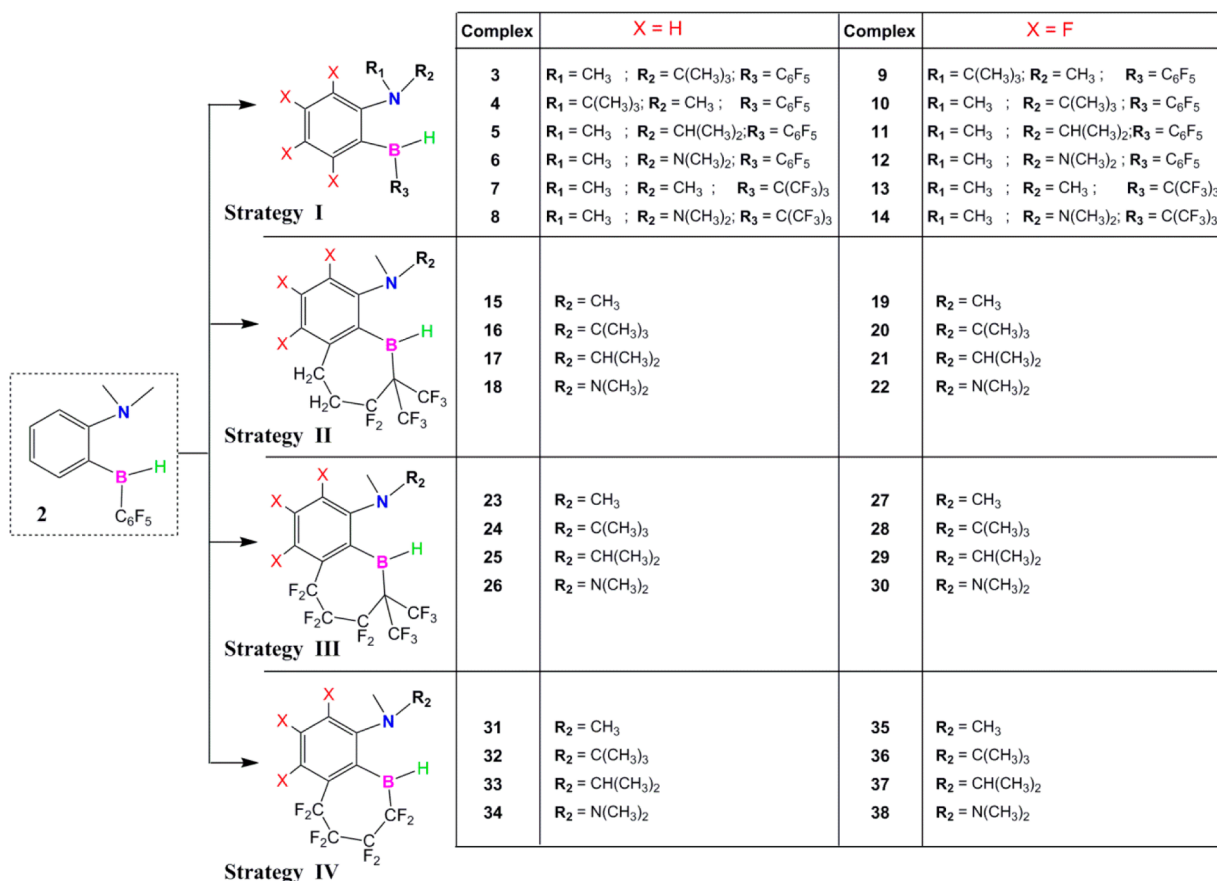


Figure 5. Four strategies that have been employed in investigating the conversion of the existing catalyst system, **2**, to potential new complexes for alcohol dehydrogenation.

Table 1. First and Second Barriers of the Catalytic Cycle for the Dehydrogenation of 1-Phenylethanol by a Range of Different FLP Complexes Considered in This Study (all values in kilocalories per mole)

complex	$(\Delta G)^\ddagger$		complex	$(\Delta G)^\ddagger$	
	TS ₁	TS ₂		TS ₁	TS ₂
8	27.9	16.8	29	28.4	16.9
15	30.2	18.9	30	17.5	3.9
18	21.7	10.2	31	24.3	15.5
19	30.0	16.4	34	22.0	10.4
22	23.9	7.4	35	21.9	12.5
25	26.8	16.3	38	21.5	9.7
26	18.3	3.7			

with a fluorinated backbone is shown in Figure S11 of the Supporting Information.

Before discussing the results obtained from the four strategies mentioned above, we here note a point regarding the slowest step for the reaction cycle for the alcohol dehydrogenation catalysis. The complete catalytic cycle for the dehydrogenation of 1-phenylethanol is shown in the Figures 3 and 4 for the case of **2** and the iridium system, respectively. As shown in the figures, the cycle involves two steps, along with the respective barriers. The first step is the extraction of the hydrogens from the alcohol, leading to the formation of the ketone, while the second step involves the formation of the dihydrogen molecule, H₂, from the hydrogenated catalyst, thereby regenerating the catalyst (see Figure

3). As shown in Figure 3, the first barrier is 16.8 kcal/mol higher than the second barrier. This higher activation barrier for the first step in comparison to the second is seen to be the trend for a range of other different systems that we have considered. As shown in Table 1, the difference between the first and second barriers is always significant [in the range of 8.8–16.5 kcal/mol (see Table 1)] for every case considered.

The reasons for this are twofold. (1) The first barrier involves the interaction of two molecular species; i.e., it is an intermolecular reaction. This leads to a higher entropic cost for the reaction, thereby increasing the barrier. (2) The crossing of the first barrier leads to an intermediate that has an energy higher than that of the reactant intermediate, while the crossing of the second barrier leads to an intermediate that has an energy lower than that of the corresponding reactant intermediate. Thus, the favorability of the second reaction leads to a reduction in the second barrier.

Because all the different representative cases discussed in Table 1 have the second barrier lower than the first, it is clear that the rate-determining step for the dehydrogenation reaction is the first step, involving the dehydrogenation of the 1-phenylethanol to the corresponding ketone. Therefore, only the first step has been considered for all the different cases that have been studied as modifications to **2** in strategies I–IV. This has been done to reduce the computational cost of doing the full quantum chemical calculations for the many FLP complexes considered in this study.

The results from the different strategies adopted are discussed below.

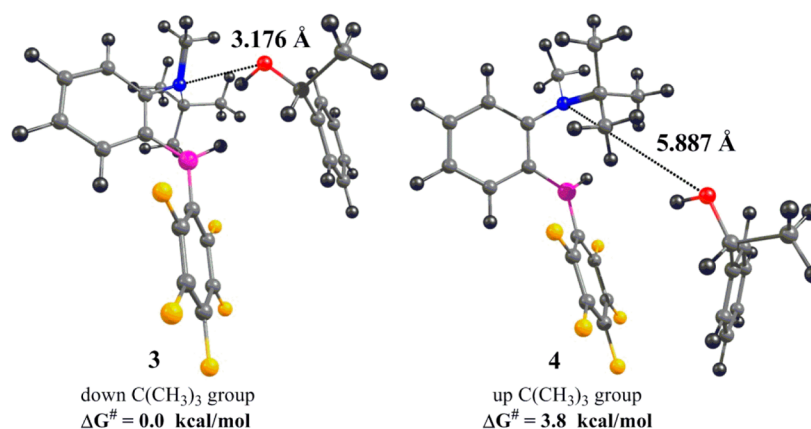


Figure 6. Comparison of the nitrogen–oxygen distances for two FLP cases: complexes 3 and 4. The color scheme is as follows: carbon, gray; nitrogen, blue; hydrogen, black; boron, pink; fluorine, yellow.

Table 2. Barrier Heights (ΔG values) for the Slowest Step of the Dehydrogenation of 1-Phenylethanol by the Newly Designed Complexes Discussed under Strategy I (all values are in kilocalories per mole)

Complex		TS_1 (ΔG) [#]
	X = H	
3	R ₁ = CH ₃ ; R ₂ = C(CH ₃) ₃ ; R ₃ = C ₆ F ₅	31.7
4	R ₁ = C(CH ₃) ₃ ; R ₂ = CH ₃ ; R ₃ = C ₆ F ₅	35.5
5	R ₁ = CH ₃ ; R ₂ = CH(CH ₃) ₂ ; R ₃ = C ₆ F ₅	28.2
6	R ₁ = CH ₃ ; R ₂ = N(CH ₃) ₂ ; R ₃ = C ₆ F ₅	28.3
7	R ₁ = CH ₃ ; R ₂ = CH ₃ ; R ₃ = C(CF ₃) ₃	33.5
8	R ₁ = CH ₃ ; R ₂ = N(CH ₃) ₂ ; R ₃ = C(CF ₃) ₃	27.9
	X = F	
9	R ₁ = C(CH ₃) ₃ ; R ₂ = CH ₃ ; R ₃ = C ₆ F ₅	41.5
10	R ₁ = CH ₃ ; R ₂ = C(CH ₃) ₃ ; R ₃ = C ₆ F ₅	34.8
11	R ₁ = CH ₃ ; R ₂ = CH(CH ₃) ₂ ; R ₃ = C ₆ F ₅	36.9
12	R ₁ = CH ₃ ; R ₂ = N(CH ₃) ₂ ; R ₃ = C ₆ F ₅	33.3
13	R ₁ = CH ₃ ; R ₂ = CH ₃ ; R ₃ = C(CF ₃) ₃	41.2
14	R ₁ = CH ₃ ; R ₂ = N(CH ₃) ₂ ; R ₃ = C(CF ₃) ₃	31.5

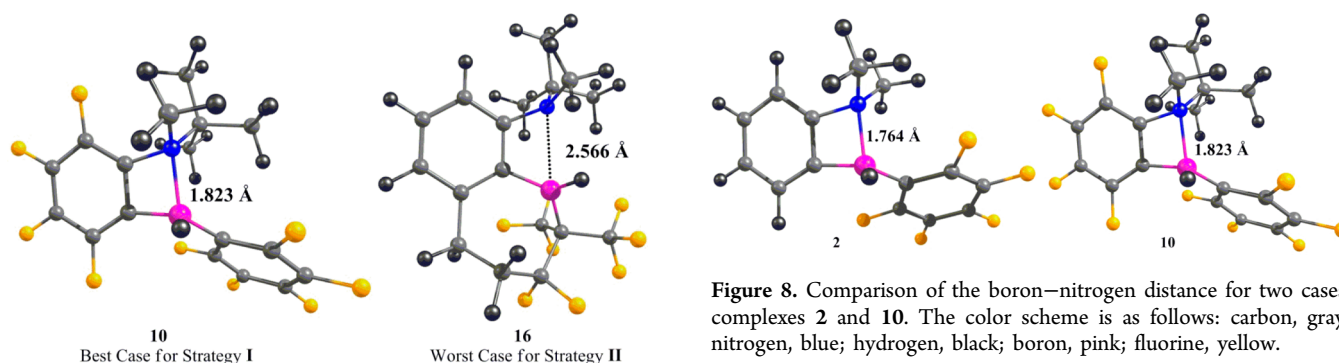


Figure 7. Comparison of the boron–nitrogen distance for two cases, complexes 10 and 16. The color scheme is as follows: carbon, gray; nitrogen, blue; hydrogen, black; boron, pink; fluorine, yellow.

Strategy I. The barriers (ΔG values) for the slowest (first) step of the reaction are listed in Table 2 for all the cases considered under strategy 1. All the barriers for the alcohol dehydrogenation reaction are seen to be quite high, in the

Figure 8. Comparison of the boron–nitrogen distance for two cases, complexes 2 and 10. The color scheme is as follows: carbon, gray; nitrogen, blue; hydrogen, black; boron, pink; fluorine, yellow.

range of 27.9–41.5 kcal/mol. Because the barriers are significantly higher than that for the iridium-based system (21.9 kcal/mol), this indicates that these FLP complexes, if synthesized, would be significantly less effective than the iridium-based system for the alcohol dehydrogenation. It is to be noted that for every case studied, its corresponding complex, in which the hydrogens were replaced with fluorines, was also considered as a potential candidate for the alcohol dehydrogenation.

Table 3. Barrier Heights (ΔG values) for the Slowest Step of the Dehydrogenation of 1-Phenylethanol by the Newly Designed Complexes Discussed under Strategy II (all values are in kilocalories per mole)

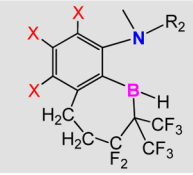
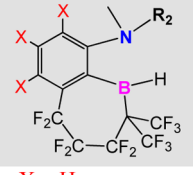
Complex		TS_1 (ΔG) [#]
	X = H	
15	R ₂ = CH ₃	30.2
16	R ₂ = C(CH ₃) ₃	33.7
17	R ₂ = CH(CH ₃) ₂	27.9
18	R ₂ = N(CH ₃) ₂	21.7
	X = F	
19	R ₂ = CH ₃	29.6
20	R ₂ = C(CH ₃) ₃	33.2
21	R ₂ = CH(CH ₃) ₂	29.1
22	R ₂ = N(CH ₃) ₂	23.9

Table 4. Barrier Heights (ΔG values) for the Slowest Step of the Dehydrogenation of 1-Phenylethanol by the Newly Designed Complexes Discussed under Strategy III (all values are in kilocalories per mole)

Complex		TS_1 (ΔG) [#]
	X = H	
23	R ₂ = CH ₃	31.1
24	R ₂ = C(CH ₃) ₃	32.8
25	R ₂ = CH(CH ₃) ₂	26.8
26	R ₂ = N(CH ₃) ₂	18.3
	X = F	
27	R ₂ = CH ₃	31.2
28	R ₂ = C(CH ₃) ₃	33.8
29	R ₂ = CH(CH ₃) ₂	28.4
30	R ₂ = N(CH ₃) ₂	17.5

ation catalysis reaction. It is seen that this did not lead to any improvement in the barrier heights for any of the cases investigated (see Table 2).

It is to be noted that different conformations can be considered for the FLP complexes that have been studied under strategy I. As shown in Figure 6, for FLP complex 3, the R₁ group is *cis* to the backbone phenyl group [denoted “down

C(CH₃)₃ group” in Figure 6], while for FLP 4, it is *trans* to the backbone phenyl group [denoted “up C(CH₃)₃ group”]. The calculations indicate that the “down” R₁ group case is the more energetically favorable conformer. In the cases of FLPs 3 and 4, the difference in energy between the two conformers is 1.7 kcal/mol, with the “down” conformer being more stable. The reason for this is steric: having the C(CH₃)₃ group *cis* to the backbone phenyl increases the distance from this bulky group to the boron center, thereby making the conformer more sterically favorable. It is also observed that for 3, the approach of the substrate alcohol is more favored in comparison to that for 4, by 3.8 kcal/mol. The reason for this is that the undesired interaction between the substrate and the C(CH₃)₃ group is minimized in the “down” conformer in comparison to the “up” conformer. As shown in Figure 6, the optimized structures of the reactant complexes of the two conformers with the substrate present show that the distance between the oxygen of the incoming alcohol and the nitrogen center is significantly lower for the “down” conformer than for the “up” conformer. This indicates that putting the bulky group *cis* to the backbone phenyl or FLP complexes would yield lower barriers for the cases considered under strategy I. Hence, for the other complexes that have been considered under this strategy, the bulkier group on the nitrogen has been kept *cis* to the phenyl ring, i.e., in the “down” conformers, which can be seen in Table 2.

These results indicate that changing the functional groups on the Lewis acidic boron and the Lewis basic nitrogen centers in the FLP is not enough to reduce the barrier for the alcohol dehydrogenation reaction, thereby implying that a different strategy has to be adopted to bring down the barrier. This is discussed in the next section, which discusses the results of employing strategy II.

Strategy II. The results from the previous section, in which 2 was modified by putting different functional groups at the boron and nitrogen centers, suggest that this is not adequate to bring about the desired changes in the rate-determining step for the alcohol dehydrogenation process. The reason the barrier heights are quite high for such cases is that there is a significant interaction between the Lewis acidic boron and the Lewis basic nitrogen centers. As shown in Figure 8, the distance between N and B is 1.764 Å in 2. For the modifications discussed in strategy I, this distance is increased by only ~0.059 Å for the best case, in terms of the greatest increase in the B–N bond distance (for the case where R₁ = CH₃, R₂ = C(CH₃)₃, and R₃ = C₆F₅, complex 10). Now, the slowest (first) step involves the addition of a hydrogen each at the nitrogen and the boron centers, which would occur at the cost of the interaction

Table 5. NBO Charge Analysis of the First Transition State for Different FLP Complexes Obtained from Strategies II and III

entry	complex	boron (B)	nitrogen (N)	$\Delta(B-N)$	complex	boron (B)	nitrogen (N)	$\Delta(B-N)$	difference (ΔG) ^{#a}
1	15	0.0646	-0.4153	0.4799	23	0.0244	-0.4292	0.4536	-0.9
2	16	0.1341	-0.4577	0.5918	24	0.0478	-0.4659	0.5137	0.9
3	17	0.1143	-0.4329	0.5472	25	0.0284	-0.4448	0.4732	1.1
4	18	0.0704	-0.2874	0.3578	26	-0.0339	-0.2981	0.2642	3.4
5	19	0.0210	-0.4177	0.4387	27	-0.0129	-0.4318	0.4189	-1.6
6	20	0.0542	-0.4564	0.5106	28	-0.0079	-0.4687	0.4608	-0.6
7	21	0.0605	-0.4342	0.4947	29	-0.0073	-0.4469	0.4396	0.7
8	22	0.0432	-0.3017	0.3449	30	-0.0748	-0.3016	0.2268	6.4

^aThis is the difference in the barrier height between the barrier obtained for the first transition state for the FLP in column 2 in comparison to the first transition state barrier for the corresponding FLP in column 6.

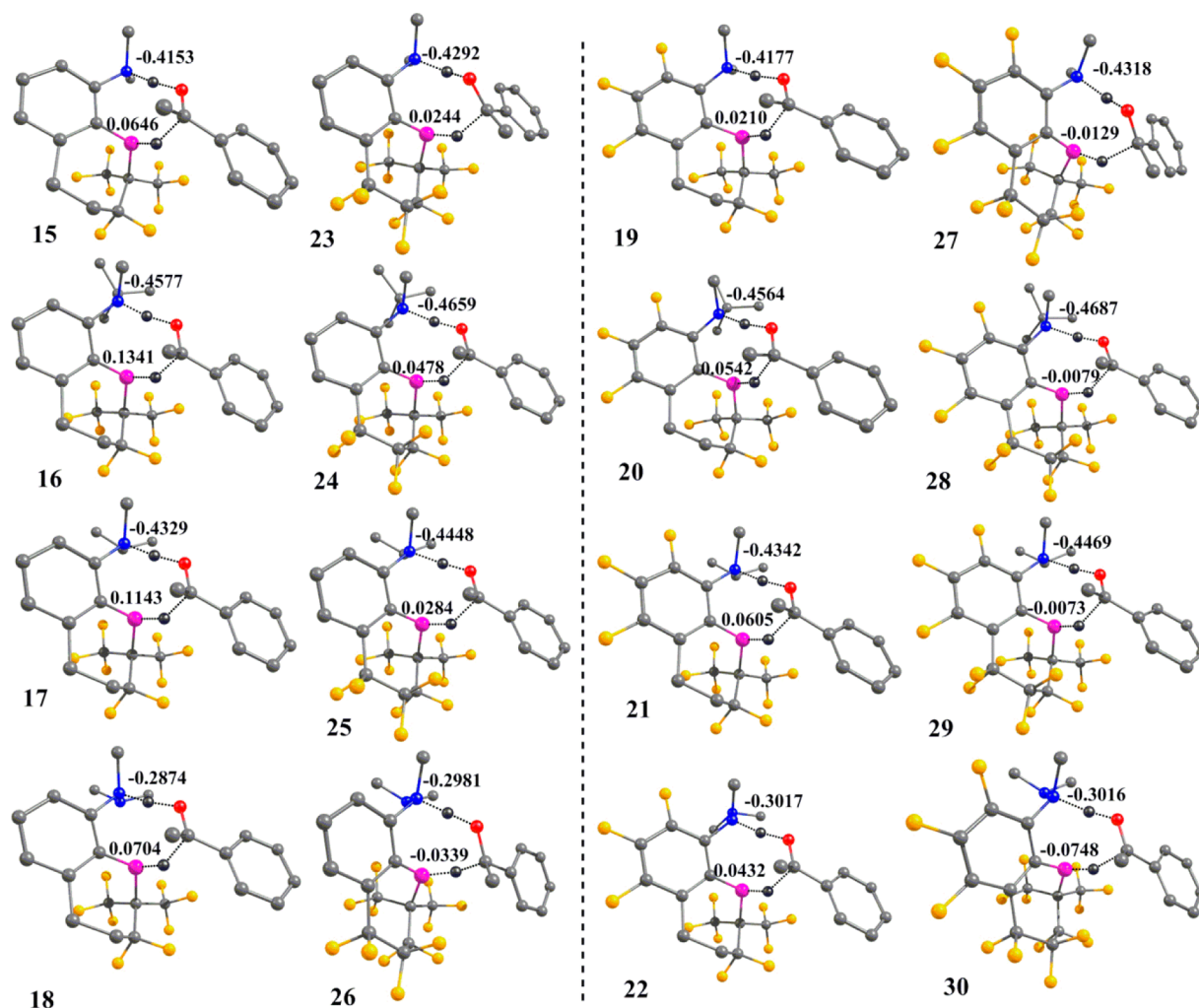


Figure 9. Comparison of the charges in the nitrogen (blue) and boron (pink) atoms in the optimized transition state structures for corresponding structures taken from the strategy II and strategy III classes. The structures on the left (15–18 and 19–22) are from strategy II, and the structures on the right (23–26 and 27–30) are from strategy III.

between the nitrogen and the boron in the FLP. Hence, any strategy that can lead to a decrease in the level of interaction between the N and B centers would lead to a decrease in the barrier. This forms the basis for strategy II, which involves the linking of the boron and the backbone phenyl group. In this manner, the level of interaction between the boron and the nitrogen centers is reduced. The linker that has been employed to connect the boron and the phenyl carbon is $\text{C}(\text{CF}_3)_2\text{-CF}_2\text{-CH}_2\text{-CH}_2$. This linker has been chosen to maximize the withdrawal of electron density from the boron center, by putting fluorine atoms in place of hydrogens in the first two carbons attached to the boron.

Figure 7 shows a comparison of the best case under strategy I, in terms of the greatest increase in the B–N bond distance, with the worst case, among all the different linked cases studied in strategy II [the case in which $\text{R}_1 = \text{CH}_3$ and $\text{R}_2 = \text{C}(\text{CH}_3)_3$, complex 16]. We observed that the B–N distance is significantly increased by linking the boron to the phenyl backbone. The N–B distance is 2.566 Å in the worst strategy II FLP case, while it is 1.823 Å in the best strategy I FLP case. This decrease in the level of interaction between the B and the N centers, i.e., the increase in the level of steric frustration in the FLP in the strategy II FLP cases, should lead to greater interaction with the hydrogens of the 1-phenylethanol

substrate, which could lead to a decrease in the dehydrogenation barrier.

This is indeed borne out by the calculations for all the different FLPs that have been considered in strategy II, as shown in Table 3. In almost every case, the barriers have dropped significantly in comparison to the barriers that have been obtained for the complexes studied under strategy I. Also, as had been done for all the cases studied under strategy I, we have considered the effect of replacing the hydrogens of the backbone phenyl ring with fluorines for all the cases considered in strategy II. The results, as shown in Table 3, indicate that this has an only marginal effect on the barriers in comparison to the corresponding nonfluorinated cases, with the barrier decreasing in two cases and increasing in the other two. This implies that fluorinating the backbone phenyl ring is unlikely to have a significant effect on the barrier heights for the alcohol dehydrogenation reaction for the cases considered under strategy II, as well.

A perusal of the results in Table 3 indicates that the most effective FLP among the ones considered in strategy II is 18, the case in which $\text{R}_2 = \text{N}(\text{CH}_3)_2$. For this, the rate-determining barrier has been found to be 21.7 kcal/mol. This compares very favorably with the barrier obtained for the iridium catalyst complex (21.9 kcal/mol). This suggests that FLP complexes

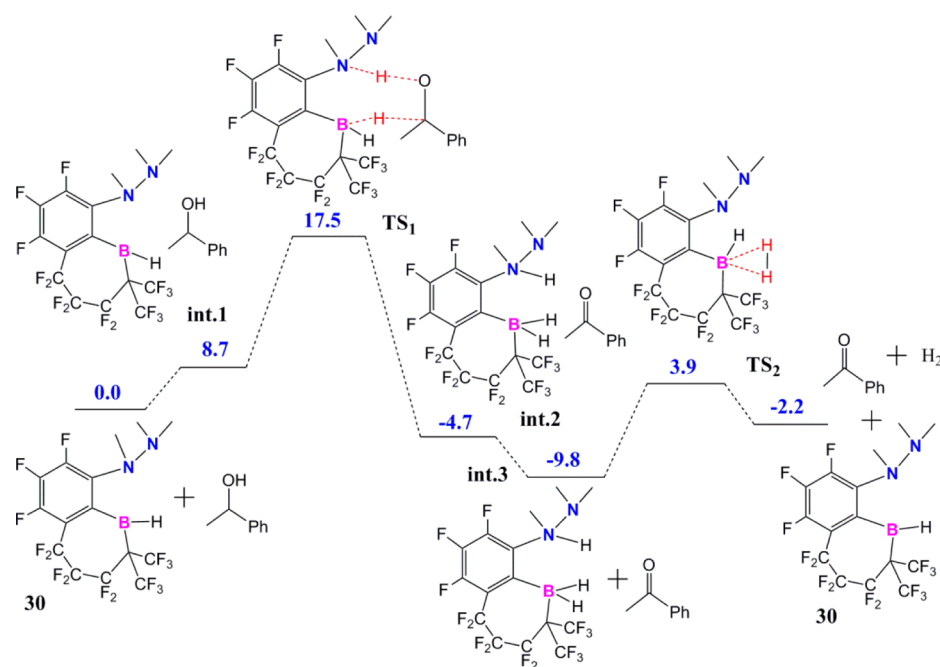


Figure 10. Free energy surface for the alcohol dehydrogenation reaction employing complex **30**. All values of free energies are given in kilocalories per mole.

Table 6. Barrier Heights (ΔG values) for the Slowest Step of the Dehydrogenation of 1-Phenylethanol by the Newly Designed Complexes Discussed under Strategy IV (all values are in kilocalories mole)

Complex	Structure	TS_1 (ΔG) [#]
	X = H	
31	R ₂ = CH ₃	24.3
32	R ₂ = C(CH ₃) ₃	27.0
33	R ₂ = CH(CH ₃) ₂	25.8
34	R ₂ = N(CH ₃) ₂	22.0
	X = F	
35	R ₂ = CH ₃	21.9
36	R ₂ = C(CH ₃) ₃	28.9
37	R ₂ = CH(CH ₃) ₂	27.4
38	R ₂ = N(CH ₃) ₂	21.5

like **18** would be as effective as the highly efficient iridium complex in catalyzing the dehydrogenation of 1-phenylethanol.

The next section will discuss modifications to the linker connecting the boron center to the phenyl backbone.

Strategy III. The previous section discussed how connecting the boron and the phenyl backbone of **2** with the C(CF₃)₂-CF₂-CH₂-CH₂ linker led to a significant decrease in the barrier height for the first step of the catalytic cycle, for almost all the cases considered. What is discussed in this section is the possibility of reducing the barriers even further by fluorinating all the hydrogens of the linker, i.e., by employing the linker C(CF₃)₂-CF₂-CF₂-CF₂. The cases, otherwise, are the same as those considered in strategy II, in terms of the R₁-R₃ groups. The values, listed in Table 4, show that the barrier increases marginally by approximately 0.6–1.6 kcal/mol in three cases (case **23** in comparison to case **15**, case **27** in comparison to

case **19**, and case **28** in comparison to case **20**). However, for the five remaining cases, the replacement of hydrogens with fluorine atoms is seen to lead to a decrease in the rate-determining barrier heights. The most important cases in this regard are **26** and **30**, in which the barrier heights are reduced to 18.3 and 17.5 kcal/mol, respectively.

An explanation for the slight increase in the barrier in some cases and the lowering of the barrier in others when corresponding cases are considered between strategies II and III is provided in Table 5 and Figure 9. An NBO charge analysis has been conducted for the nitrogen and the boron atoms in the transition state structures for the first transition state for the corresponding cases taken from strategies II and III. It is seen that the difference in charge between the N and the B atoms is almost the same between corresponding cases where the barrier is only slightly increased between strategies II and III (see Table 5, entries 1, 5, and 6). However, for the five strategy III cases in which the barriers are lowered, it is observed that there is a marked reduction in the difference in charge between the N and the B atoms (see Table 5, entries 2–4, 7, and 8). This indicates that the level of electrostatic interaction between the two atoms is reduced in these five strategy III cases in comparison to that of their strategy II counterparts, in the transition state structures. This would lead to greater ease of separation between the N and the B atoms, thereby reducing the barrier.

Of all 36 cases that have been proposed and studied in this computational investigation, **30** represents the case that would be predicted to be the most efficient at conducting the alcohol dehydrogenation catalysis. The complete catalytic cycle for the dehydrogenation of 1-phenylethanol by **30** is shown in Figure 10. As discussed earlier, the reactions subsequent to the first step proceed with very little further requirement of energy, with the second barrier being only 13.7 kcal/mol for the case of this FLP.

The values for the barrier heights for the slowest step for alcohol dehydrogenation for **26** and **30** are 3.6 and 4.4 kcal/

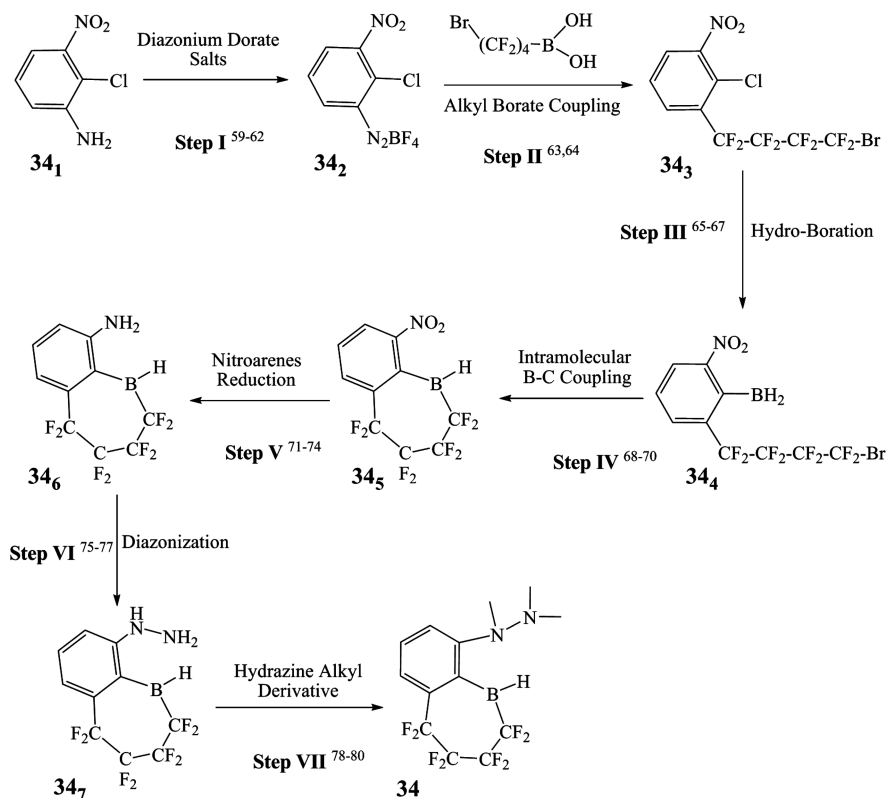


Figure 11. Proposed synthesis of complex 34.

mol lower, respectively, than the corresponding barrier height for the iridium catalyst case. Hence, the current computational investigations provide a pointer with respect to how non-metal-based FLPs can be improved to make them significantly better than the state-of-the-art metal-based systems in conducting important chemical transformations.

Strategy IV. The last strategy that has been investigated is to reduce the size of the linker by replacing the $C(CF_3)_2-CF_2-CF_2-CF_2$ linker employed in strategy III with the $CF_2-CF_2-CF_2-CF_2$ linker. This replacement of the CF_3 groups in the carbon α to the boron with the smaller fluorine atoms has been conducted to reduce the likelihood of steric interactions between the CF_3 groups and the hydrogens of the incoming alcohol substrate. That this change has a salutary effect on the barrier heights is evidenced by the results, listed in Table 6. The barrier heights are reduced to the range of 21.5–28.9 kcal/mol for the eight cases considered. Indeed, the investigation of these cases throws up three new possible FLPs, 38, 35, and 34, that have barrier heights for the slowest step (21.5, 21.9, and 22.0 kcal/mol, respectively) that are comparable to the corresponding barrier height for the iridium catalyst case (21.9 kcal/mol). This suggests that this strategy of employing a simpler linker can also lead to effective FLPs for alcohol dehydrogenation catalysis.

Overall, the current computational investigations indicate that one can design new FLPs beginning from an existing, experimentally synthesized FLP and introduce modifications that can increase the efficiency of the FLP substantially. As shown in the graph in Figure 11, of the 36 cases investigated, there are six (18, 26, 30, 34, 35, and 38) that compare very favorably with the iridium catalyst, which is the state-of-the-art system present today for alcohol dehydrogenation catalysis.¹¹ It is to be noted that five of the six cases (18, 26, 30, 34, and 38)

feature an N–N bond in the FLP. It is likely that the presence of the nitrogen attached to the Lewis basic FLP nitrogen increases its Lewis basicity and thereby leads to a reduction in the barrier. Because N/B FLPs having an N–N substitution have not yet been reported, a synthetic route to making such complexes is shown in Figure 11 for FLP case 34. It is possible that such FLPs may also face decomposition pathways during the catalysis reaction, but such possibilities are beyond the scope of this work.

This result also indicates the importance of modifying FLPs to increase the steric hindrance between the Lewis acid and base moieties in the FLP, thereby increasing their capacity to conduct new chemistry. The complete catalytic cycles for the dehydrogenation of 1-phenylethanol for cases 18, 26, 34, 35, and 38 are shown in Figures S2–S6 of the Supporting Information.

CONCLUSIONS

Full quantum chemical calculations have been conducted by employing density functional theory (DFT) to test the possibility of designing new chemical systems that can do the important catalytic conversion of alcohols to the corresponding ketones. Specifically, metal free systems have been considered, based on the frustrated Lewis pair (FLP) concept that has recently been developed.²⁸ Different strategies have been considered to design new FLPs beginning from an existing, experimentally synthesized FLP,⁵¹ a complex having a weak nitrogen–boron interaction that can be ruptured and regenerated during the alcohol dehydrogenation catalysis process. Careful investigations with 36 proposed FLP complexes reveal that new FLPs can be designed with a weaker interaction between the nitrogen and boron centers, which can thereby lead to systems that would be very effective

at the alcohol dehydrogenation process. Indeed, there are several metal free FLP cases that have been identified in this work that would have barriers comparable to or lower than the calculated barrier for the slowest step for the state-of-the-art acceptorless alcohol dehydrogenation (AAD) metal catalyst present today (Figure 12).¹¹

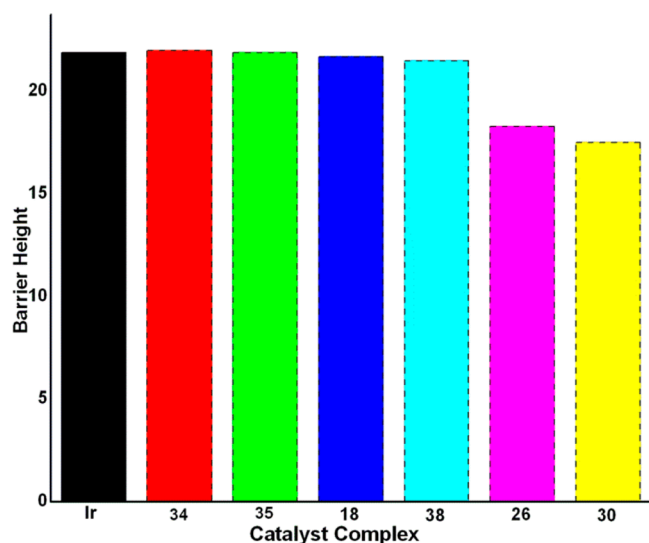


Figure 12. Comparison of the barrier heights for the slowest step of the alcohol dehydrogenation process for the six best FLP complexes obtained from this study with the corresponding barrier height for the state-of-the-art iridium catalyst.

This work, therefore, provides insight into how one can substitute highly effective transition metal-based alcohol dehydrogenation catalyst systems with cheaper and greener metal free catalysts and should thus serve as a guide for experimentalists working in this important area of research.

■ ASSOCIATED CONTENT

📄 Supporting Information

Structures and free energy surfaces (Figures S1–S11) and Cartesian coordinates of all the intermediates and transition states mentioned in this work. This material is available free of charge via the Internet at <http://pubs.acs.org>.

■ AUTHOR INFORMATION

Corresponding Author

*E-mail: k.vanka@ncl.res.in

Notes

The authors declare no competing financial interest.

■ ACKNOWLEDGMENTS

Funding from the FP7-NMP-EU-India-2 collaborative project HYPOMAP on “New Materials for Hydrogen Powered Mobile Applications” is gratefully acknowledged. The authors also thank the Centre of Excellence in Scientific Computing (COESC), NCL, Pune, for providing computational facilities. K.V. is grateful to the Department of Science and Technology (DST) for financial assistance. The authors also acknowledge the Multi-Scale Simulation and Modeling project (MSM) for providing financial assistance.

■ REFERENCES

- (1) Tojo, G.; Fernandez, M. *Oxidation of Alcohols to Aldehydes and Ketones*; Springer: New York, 2006.
- (2) Hudlicky, M. *Oxidations in Organic Chemistry*; American Chemical Society: Washington, DC, 1990.
- (3) Watson, A. J. A.; Williams, J. M. J. *Science* **2010**, *329*, 635–636.
- (4) Fujita, K.-i.; Yamaguchi, R. *Synlett* **2005**, 560–571.
- (5) Nath, K.; Das, D. *Curr. Sci.* **2003**, *85*, 265–271.
- (6) Navarro, R. M.; Peña, M. A.; Fierro, J. L. G. *Chem. Rev.* **2007**, *107*, 3952–3991.
- (7) Piscina, P. R. d. l.; Homs, N. *Chem. Soc. Rev.* **2008**, *37*, 2459–2467.
- (8) Balat, H.; Kirtay, E. *Int. J. Hydrogen Energy* **2010**, *35*, 7416–7426.
- (9) Zhang, J.; Gandelman, M.; Shimon, L. J. W.; Rozenberg, H.; Milstein, D. *Organometallics* **2004**, *23*, 4026–4033.
- (10) van Buijtenen, J.; Meuldijk, J.; Vekemans, J. A. J. M.; Hulshof, L. A.; Kooijman, H.; Spek, A. L. *Organometallics* **2006**, *25*, 873–881.
- (11) Li, H.; Lu, G.; Jiang, J.; Huang, F.; Wang, Z.-X. *Organometallics* **2011**, *30*, 2349–2363.
- (12) Gunanathan, C.; Milstein, D. *Science* **2013**, *341*, 249.
- (13) Marko, I. E.; Giles, P. R.; Tsukazaki, M.; Brown, S. M.; Urch, C. J. *Science* **1996**, *274*, 2044–2046.
- (14) Hayashi, M.; Kawabata, H. *J. Synth. Org. Chem Jpn.* **2002**, *60*, 137–144.
- (15) Sheldon, R. A.; Arends, I. W. C. E.; ten Brink, G.-J.; Dijkstra, A. *Acc. Chem. Res.* **2002**, *35*, 774–781.
- (16) Sigman, M. S.; Jensen, D. R. *Acc. Chem. Res.* **2006**, *39*, 221–229.
- (17) Gligorich, K. M.; Sigman, M. S. *Chem. Commun.* **2009**, 3854–3867.
- (18) Noyori, R.; Aoki, M.; Sato, K. *Chem. Commun.* **2003**, 1977–1986.
- (19) Piera, J.; Bäckvall, J.-E. *Angew. Chem., Int. Ed.* **2008**, *47*, 3506–3523.
- (20) Gharah, N.; Chakraborty, S.; Mukherjee, A. K.; Bhattacharyya, R. *Inorg. Chim. Acta* **2009**, *362*, 1089–1100.
- (21) Almeida, M. L. S.; Beller, M.; Wang, G.-Z.; Bäckvall, J.-E. *Chem.—Eur. J.* **1996**, *2*, 1533–1536.
- (22) Hanasaka, F.; Fujita, K.-i.; Yamaguchi, R. *Organometallics* **2005**, *24*, 3422–3433.
- (23) Dobereiner, G. E.; Crabtree, R. H. *Chem. Rev.* **2010**, *110*, 681–703.
- (24) Hamid, M. H. S. A.; Williams, J. M. J. *Chem. Commun.* **2007**, 725–727.
- (25) Nixon, T. D.; Whittlesey, M. K.; Williams, J. M. J. *Dalton Trans.* **2009**, 753–762.
- (26) Yamaguchi, R.; Ikeda, C.; Takahashi, Y.; Fujita, K.-i. *J. Am. Chem. Soc.* **2009**, *131*, 8410–8412.
- (27) Fujita, K.-i.; Tanino, N.; Yamaguchi, R. *Org. Lett.* **2007**, *9*, 109–111.
- (28) Welch, G. C.; Juan, R. R. S.; Masuda, J. D.; Stephan, D. W. *Science* **2006**, *314*, 1124–1126.
- (29) Stephan, D. W.; Erker, G. *Chem. Sci.* **2014**, *5*, 2625–2641.
- (30) Sajid, M.; Elmer, L.-M.; Rosorius, C.; Daniliuc, C. G.; Grimme, S.; Kehr, G.; Erker, G. *Angew. Chem., Int. Ed.* **2013**, *52*, 2243–2246.
- (31) Rokob, T. A.; Hamza, A.; Stirling, A.; Soós, T.; Pápai, I. *Angew. Chem., Int. Ed.* **2008**, *47*, 2435–2438.
- (32) Sumerin, V.; Schulz, F.; Nieger, M.; Leskelä, M.; Repo, T.; Rieger, B. *Angew. Chem., Int. Ed.* **2008**, *47*, 6001–6003.
- (33) Miller, A. J. M.; Bercaw, J. E. *Chem. Commun.* **2010**, 46, 1709–1711.
- (34) Zhao, L.; Lu, G.; Huang, F.; Wang, Z.-X. *Dalton Trans.* **2012**, *41*, 4674–4684.
- (35) Greb, L.; Oña-Burgos, P.; Schirmer, B.; Grimme, S.; Stephan, D. W.; Paradies, J. *Angew. Chem., Int. Ed.* **2012**, *51*, 10164–10168.
- (36) Zhao, L.; Li, H.; Lu, G.; Wang, Z.-X. *Dalton Trans.* **2010**, *39*, 4038–4047.
- (37) Chase, P. A.; Welch, G. C.; Jurca, T.; Stephan, D. W. *Angew. Chem., Int. Ed.* **2007**, *46*, 8050–8053.

- (38) Sumerin, V.; Schulz, F.; Atsumi, M.; Wang, C.; Nieger, M.; Leskelä, M.; Repo, T.; Pyykko, P.; Rieger, B. *J. Am. Chem. Soc.* **2008**, *130*, 14117–14119.
- (39) Chase, P. A.; Jurca, T.; Stephan, D. W. *Chem. Commun.* **2008**, 1701–1703.
- (40) Li, H.; Zhao, L.; Lu, G.; Huang, F.; Wang, Z.-X. *Dalton Trans.* **2010**, *39*, 5519–5526.
- (41) Privalov, T. *Chem.—Eur. J.* **2009**, *15*, 1825–1829.
- (42) Guo, Y.; He, X.; Li, Z.; Zou, Z. *Inorg. Chem.* **2010**, *49*, 3419–3423.
- (43) Welch, G. C.; Stephan, D. W. *J. Am. Chem. Soc.* **2007**, *129*, 1880–1881.
- (44) Spies, P.; Erker, G.; Kehr, G.; Bergander, K.; Frohlich, R.; Grimme, S.; Stephan, D. W. *Chem. Commun.* **2007**, 5072–5074.
- (45) McCahill, J. S. J.; Welch, G. C.; Stephan, D. W. *Angew. Chem., Int. Ed.* **2007**, *46*, 4968–4971.
- (46) Guo, Y.; Li, S. *Eur. J. Inorg. Chem.* **2008**, *2008*, 2501–2505.
- (47) Guo, Y.; Li, S. *Inorg. Chem.* **2008**, *47*, 6212–6219.
- (48) Stirling, A.; Hamza, A.; Rokob, T. A.; Papai, I. *Chem. Commun.* **2008**, 3148–3150.
- (49) Staubitz, A.; Besora, M.; Harvey, J. N.; Manners, I. *Inorg. Chem.* **2008**, *47*, 5910–5918.
- (50) Chernichenko, K.; Nieger, M.; Leskela, M.; Repo, T. *Dalton Trans.* **2012**, *41*, 9029–9032.
- (51) Chernichenko, K.; Madarász, A.; Pápai, I.; Nieger, M.; Leskela, M.; Repo, T. *Nat. Chem.* **2013**, *5*, 718–723.
- (52) Ahlrichs, R.; Baer, M.; Haeser, M.; Horn, H.; Koelmel, C. *Chem. Phys. Lett.* **1989**, *162*, 165.
- (53) Perdew, J. P.; Burke, K.; Ernzerhof, M. *Phys. Rev. Lett.* **1996**, *77*, 3865.
- (54) Eichkorn, K.; Treutler, O.; Öhm, H.; Häser, M.; Ahlrichs, R. *Chem. Phys. Lett.* **1995**, *240*, 283–289.
- (55) Sierka, M.; Hogekamp, A.; Ahlrichs, R. *J. Chem. Phys.* **2003**, *118*, 9136.
- (56) Becke, A. D. *J. Chem. Phys.* **1993**, *98*, 5648–5652.
- (57) Lee, C.; Yang, W.; Parr, R. G. *Phys. Rev. B* **1988**, *37*, 785–789.
- (58) Grimme, S. *J. Comput. Chem.* **2006**, *27*, 1787–1799.
- (59) Matheis, C.; Jouvin, K.; Goossen, L. J. *Org. Lett.* **2014**, *16*, 5984–5987.
- (60) Darses, S.; Michaud, G.; Genêt, J.-P. *Eur. J. Org. Chem.* **1999**, 1999, 1875–1883.
- (61) Doyle, M. P.; Bryker, W. J. *J. Org. Chem.* **1979**, *44*, 1572–1574.
- (62) Colas, C.; Goelder, M. *Eur. J. Org. Chem.* **1999**, 1999, 1357–1366.
- (63) Andrus, M. B.; Song, C. *Org. Lett.* **2001**, *3*, 3761–3764.
- (64) Sengupta, S.; Bhattacharyya, S. *J. Org. Chem.* **1997**, *62*, 3405–3406.
- (65) Franz, D.; Bolte, M.; Lerner, H.-W.; Wagner, M. *Dalton Trans.* **2011**, *40*, 2433–2440.
- (66) Seven, Á. M.; Bolte, M.; Lerner, H.-W.; Wagner, M. *Organometallics* **2014**, *33*, 1291–1299.
- (67) Lorbach, A.; Hubner, A.; Wagner, M. *Dalton Trans.* **2012**, *41*, 6048–6063.
- (68) White, J.; Whiteley, C. G. *Synthesis* **1993**, 1993, 1141–1144.
- (69) Mikhailov, B. M.; Bubnov, Y. N.; Tsyban, A. V. *J. Organomet. Chem.* **1978**, *154*, 113–130.
- (70) Miyaura, N. *Bull. Chem. Soc. Jpn.* **2008**, *81*, 1535–1553.
- (71) Cantillo, D.; Moghaddam, M. M.; Kappe, C. O. *J. Org. Chem.* **2013**, *78*, 4530–4542.
- (72) Sabater, S.; Mata, J. A.; Peris, E. *Chem.—Eur. J.* **2012**, *18*, 6380–6385.
- (73) Park, S.; Lee, I. S.; Park, J. *Org. Biomol. Chem.* **2013**, *11*, 395–399.
- (74) Sharma, S.; Kumar, M.; Kumar, V.; Kumar, N. *J. Org. Chem.* **2014**, *79*, 9433–9439.
- (75) Coleman, G. H. *Org. Synth.* **1922**, *2*, 71–74.
- (76) Robinson, J. R.; Good, N. E. *Can. J. Chem.* **1957**, *35*, 1578–1581.
- (77) Ohno, H.; Tanaka, H.; Takahashi, T. *Synlett* **2005**, *2005*, 1191–1194.
- (78) Giumanini, A. G.; Chiavari, G.; Musiani, M. M.; Rossi, P. *Synthesis* **1980**, 743–746.
- (79) Bredihhin, A.; Maeorg, U. *Tetrahedron* **2008**, *64*, 6788–6793.
- (80) Hisler, K.; Commeureuc, A. I. G. J.; Zhou, S.-z.; Murphy, J. A. *Tetrahedron Lett.* **2009**, *50*, 3290–3293.